

**6th International Conference
on
Wind Turbine Noise
Glasgow 20-23 April 2015**

**On predicting wind turbine noise and amplitude modulation
using Amiet's theory**

Samuel Sinayoko University of Southampton, Highfield SO17 1BJ UK.

E-mail: s.sinayoko@soton.ac.uk

**Jeremy Hurault Vestas Technology UK Ltd, West Medina Mills,
Newport, Isle of Wight PO30 5TS UK.**

E-mail: jehur@vestas.com

1. Summary

Amiet's aerofoil broadband noise theory is ideally suited to modelling wind turbine noise but few attempts have been published on validating it against experimental data for a full turbine. The main objective of this paper is to present such a validation. Furthermore, slightly different versions of Amiet's theory have been published, making it unclear how to apply it. This paper first reviews and clarifies the outstanding pitfalls in the application of Amiet's theory. The theory is then used to predict the sound power level and amplitude modulation for the DAN-AERO 40m radius turbine. Both trailing edge noise and leading edge noise are considered. Finally, Amiet's theory is used to estimate amplitude modulation. In all cases, results are in good agreement with available experimental data. This paper provides an example of the flexibility and effectiveness of Amiet's theory for predicting wind turbine noise.

2. Introduction

Wind turbine noise is dominated by trailing edge noise and leading edge noise (Oerlemans and Sijtsma 2007). Both are broadband and originate from the interaction of turbulence with the wind turbine blade. This makes them difficult to predict. Direct noise predictions based on unsteady CFD are too expensive to be used in the design process. There is a need for efficient analytical models for predicting wind turbine noise.

The theory developed by Amiet provides such a model. Amiet derived blade response functions that relate the wavenumber spectrum of the incoming turbulence to the pressure jump over the blade surface (R Amiet 1975; R Amiet 1976; RK Amiet 1978). The pressure jump defines the strength of the dipoles distributed along the airfoil surface. These dipoles are efficient noise sources that can be propagated to the far field using Curle's theory (Curle 1955). A good review of Amiet's theory for isolated aerofoils is given in (R. K. Amiet 1986).

Amiet initially derived closed form expressions for the transfer functions between the wavenumber spectrum of the incoming turbulence and the noise spectrum in the far field. He later extended his theory to rotating airfoils (Schlinker and Amiet 1981). This involved applying appropriate Doppler factors. How to do so properly remained unclear until recently due to some discrepancies in the literature. This issue has recently been resolved, giving a renewed confidence and appreciation for Amiet's model (S Sinayoko, Kingan, and Agarwal 2013), which is thought to be ideally suited to predicting wind turbine noise.

Early applications of Amiet's model to wind turbine noise were made by (Glegg, Baxter, and Glendinning 1987) and (Lowson 1993). At the time, the main focus was on identifying the dominant noise source. In Glegg et al's study, inflow noise was found to be the dominant source, whereas Lowson showed that trailing edge noise should generally be dominant. A greater understanding of the dominant source mechanism was obtained thanks to a series of experimental and theoretical studies by Oerlemans et al (Sijtsma, Oerlemans, and Holthusen 2001; Oerlemans and Sijtsma 2007; Oerlemans 2009) who demonstrated that trailing edge noise was the dominant noise source. However, they did not attempt to use the full Amiet model to predict wind turbine noise (Oerlemans and Schepers 2010).

Few such attempts have been made so far. Lee et al (Lee, Lee, and Lee 2013) estimated wind turbine noise by combining Amiet's model for trailing edge noise with the Ffowcs-Williams and Hawking's equations in the time domain (Casper and Farassat 2004; Ffowcs-Williams 1963). One advantage of their method is that they obtain the pressure field in the time domain, and therefore preserve the phase information. They use this information to estimate amplitude modulation in multiple observer directions. However, they do not compare their predictions with experimental results. Furthermore, working in the time domain appears more expensive than staying in the frequency domain, and it is possible to estimate amplitude modulation directly in the frequency domain. This was recognised by (Cheong and Joseph 2014) who presented an extensive study of amplitude modulation (swishing noise) using Amiet's model. In that study, they predicted very high levels of amplitude modulation that were explained by a singularity in Amiet's acoustic lift function. This singularity may be non-physical, however, due to a numerical issue in implementing the acoustic lift that was first highlighted in (Michel Roger and Moreau 2012). It is unclear at this stage how this may have affected Cheong et al's predictions of amplitude modulation. One of the aims of this paper is to clarify this issue. Furthermore, Cheong et al's study focused on a single wind turbine and it is unclear how amplitude modulation may vary when considering multiple wind turbines.

The main objective of this paper is to fully implement Amiet's theory for both trailing edge noise and leading edge noise, and to compare the result with experimental data for a full wind turbine blade. The DAN-AERO 40m radius wind turbine blade was used as it has been already been researched extensively (Madsen et al. 2010).

This paper first gives a brief overview of Amiet's theory and highlights three key issues that can affect the application of Amiet's theory (section 3). Implementation details are discussed in section 4. Results comparing predictions to experimental data provided by Vestas, for a DAN-AERO turbine (Madsen et al. 2010) are presented in section 5. The results include sound power level comparisons, a parametric study on leading edge sound power, and ground maps of amplitude

modulation for various configurations. The results are discussed in section 6.

3. Amiet's aerofoil broadband noise theory

Trailing edge noise is generated in two steps. Hydrodynamic fluctuations convecting along the boundary layer are scattered into noise at the trailing edge. This occurs in order to satisfy the Kutta condition at the trailing edge: pressure must be continuous in the wake of the airfoil. The scattered field induces unsteady fluctuations on the blade surface, which can be regarded as a distribution of dipole sources. Dipole sources are efficient at radiating noise. However, for small acoustic wavelengths relative to the chord, most of these dipoles are distributed close to the trailing edge. This is why the sources appear to be the trailing edge of the airfoil. Similarly, leading edge noise is produced by the scattering of inflow turbulence at the leading edge of the airfoil.

A brief summary of the theory is presented hereafter for both isolated aerofoils then rotating aerofoils. For isolated aerofoils, a good review is presented in (R. K. Amiet 1986); for rotating aerofoils, detailed reviews are given in (S Sinayoko, Kingan, and Agarwal 2013; Schlinker and Amiet 1981).

3.1. Isolated aerofoil theory

Amiet showed that, assuming frozen turbulence and using Schwartzschild's theory (R. K. Amiet 1976; M Roger and Moreau 2005), it is possible to express the far field power spectral density (PSD) in the form:

$$S_{pp}(\omega) = \left(\frac{\omega}{c_0} \frac{z}{4\pi\sigma^2} \right)^2 S_{ff}(\omega), \quad (3.1.1)$$

where S_{ff} is a frequency force power spectral density, and where (X, Y, Z) denote the observer coordinates centered on the trailing edge, with X in the chordwise direction pointing downstream and Z in the vertical direction pointing upwards, and where

$$\sigma^2 = X^2 + \beta^2(Y^2 + Z^2), \quad \beta^2 = 1 - M_X^2,$$

where M_X is the flow Mach number.

For trailing edge noise, the frequency force power spectral density can be expressed as

$$S_{ff}(\omega) = \frac{1}{2} SC^2 |\Psi_{TE}(k_X, k_S, k_C)|^2 l_S(k_X, k_S) S_{qq}(\omega), \quad (3.1.2)$$

where S and C denote the blade span and chord,

$$k_X = \frac{\omega}{U_c}, \quad k_S = \frac{\omega}{c_0 \sigma}, \quad k_C = \frac{\omega}{c_0 \beta^2} \left(M_X - \frac{X}{\sigma} \right),$$

and the correlation length l_S is derived as follows (M Roger and Moreau 2005)

$$l_S(k_X, k_S) = \frac{1}{k_X} \frac{\eta}{\eta^2 + (k_S/k_X)^2}, \quad (3.1.3)$$

where η is the exponential decay rate of the spanwise coherence function. This paper uses the value $\eta = 0.62$ measured in (Brooks and Hodgson 1981) for a NACA 0012 at Mach 0.11 and zero angle of attack. In this paper, we use the model of (Kim and

George 1982) for modelling the frequency spectrum $S_{qq}(\omega)$ at the trailing edge.

For leading edge noise, the frequency force power spectral density can similarly be expressed as

$$S_{ff}(\omega) = 2\pi^3 \rho_0^2 S C^2 U_c |\Psi_{LE}(k_x, k_s, k_c)|^2 \Phi_{ww}(k_x, k_s),$$

where Φ_{ww} is defined using Karman's spectrum model (R. K. Amiet 1986)

$$\Phi_{ww} = \frac{4}{9\pi} \frac{u_{rms}^2}{k_e^2} \frac{\hat{k}x^2 + \hat{k}y^2}{(1 + \hat{k}x^2 + \hat{k}y^2)^{7/3}}$$

where u_{rms} can be expressed in terms of the turbulence intensity I as

$$u_{rms} = IM_X c_0,$$

and where the hats signify normalization by the wavenumber

$$k_e = \frac{\sqrt{\pi}}{L} \frac{\Gamma(5/6)}{\Gamma(1/3)},$$

where L is the integral length scale of the inflow turbulence and Γ denotes the Gamma function.

Note that the acoustic lift functions Ψ_{TE} and Ψ_{LE} in equations (3.1.2) and (3.1.3) are provided by Amiet in reference (R. K. Amiet 1986).

3.2. Rotating airfoil theory

Following (Schlinker and Amiet 1981; S Sinayoko, Kingan, and Agarwal 2013), the instantaneous PSD is given in source time τ as

$$S_{pp}(\underline{x}_o, \tau, \omega) = \left(\frac{\omega'}{\omega}\right)^2 S_{pp}'(\underline{X}, \tau, \omega'),$$

where ω' and S_{pp}' are the frequency and the instantaneous power spectral density in the reference frame of the source respectively.

The observer position \underline{X} is defined as

$$\underline{X} = \underline{\underline{R}}_y(\alpha) \underline{\underline{R}}_z(\pi/2 - \alpha) (\underline{x}_o - \underline{x}_p),$$

where α is the pitch angle, $\underline{x}_p \approx \underline{\underline{M}}_{BO} c_0 T_e$ is the present source position (assuming that the source is emitted at the hub, which is valid for an observer in the far field) and is expressed in terms of the blade Mach number $\underline{\underline{M}}_{BO} = M_t \hat{\underline{y}}$ relative to the observer.

$\underline{\underline{R}}_z$ and $\underline{\underline{R}}_y$ denote the rotation matrices about the z -axis and y' -axis respectively, with $\underline{y}' = \underline{\underline{R}}_z(\pi/2 - \alpha) \underline{y}$. The propagation time T_e is obtained from $R_e \equiv c_0 T_e$, where R_e is the distance from the convected (or retarded) source position to the observer location:

$$R_e = \frac{R \left(-M_z \cos \theta + \sqrt{1 - M_z^2 \sin^2 \theta} \right)}{1 - M_z^2}, \text{ (far field),}$$

where $\theta = \pi - \theta$ denotes the angle between the flow Mach number relative to the observer and \underline{x}_o .

Finally, the source frequency ω' is related to the observer frequency ω through the Doppler shift (S Sinayoko, Kingan, and Agarwal 2013)

$$\frac{\omega}{\omega'} = 1 - \frac{M_{OB} \cdot \hat{CO}}{1 + M_{FB} \cdot \hat{CO}} \text{ (far field),}$$

where $M_{FO} = -M_z \hat{z}$ is the flow Mach number relative to the observer, and $\hat{CO} = CO / |CO|$ is the unit vector from the convected source position to the observer position.

The spectrum S_{pp}' in the reference frame of the blade can be computed from equation (3.1.1), using a frequency force spectrum S_{ff} representative of trailing edge noise (equation (3.1.2)) or leading edge noise (equation (3.1.3)).

3.3. Key pitfalls

This section summarizes the outstanding pitfalls in applying Amiet's theory. For isolated aerofoils, one issue is the confusion between the incident pressure jump and the incident pressure field. For a flat plate at zero angle of attack, the incident pressure jump (or blocked pressure) for a boundary layer on one side of the plate equals twice the incident pressure field (i.e. the pressure field that would exist without the plate). Amiet expresses his theory in terms of the pressure jumps, while other authors favour the incident pressure field (Roger and Moreau 2005; Moreau and Roger 2009; Howe 1978). One advantage of the pressure jump is that it can be measured directly using surface pressure probes. Furthermore, the wavenumber spectra required in Amiet's theory are wall pressure spectra and are expressed in terms of the pressure jump. For a boundary layer on both sides of the aerofoil, one may treat each side independently since the problem is linear; at zero angle of attack, it is sufficient to double the wall pressure spectrum compared to one sided boundary layer.

A second problem is the presence of a singularity in the acoustic lift, as pointed out by (Michel Roger and Moreau 2012). A simple work around is to express the acoustic lift as

$$\Psi(k_x, k_y, k_c) = \frac{j}{A} (\sqrt{2jB} E(B - A) + \exp(2jA)(1 - \operatorname{erf}(\sqrt{2jB}))),$$

where

$$E(z) = \frac{\operatorname{erf}(\sqrt{2jz})}{\sqrt{2jz}}$$

if $z \neq 0$, and $E(0) = 2/\sqrt{\pi}$. In comparison to the usual expression for Ψ provided for example in Sinayoko et al the above expression does not become singular when $B = A$ (see the above reference for expressing A and B in terms of the input wavenumbers). This singularity may explain the super-directive behaviour of the amplitude modulation observed by (Cheong and Joseph 2014).

Finally, a third pitfall is the exponent of the Doppler shift in the rotating model. As explained by (S Sinayoko, Kingan, and Agarwal 2013), the exponent should be 1 for the instantaneous spectrum, and 2 for the time averaged spectrum. One exponent stems from expressing the PSD in two different reference frames, and another exponent stems from expressing the observer time in terms of the source time. However, this problem is not a major concern for current wind turbines for which the Mach number is small.

4. Implementation

The blade geometry is provided in the DAN-AERO final report (Madsen et al. 2010).

The point frequency spectrum of (Kim and George 1982) requires knowledge of the boundary layer momentum thickness, which is obtained for each blade section by using the panel method code X-foil. X-foil uses the local Mach number and angle of attack as inputs. These are obtained by combining measurements of the lift, drag, and momentum coefficients as a function of angle of attack, with Vesta's in-house Blade Element Momentum code PYRO 2.1.6, for a wind speed of 8.5 m/s and a tip speed ratio of 8.9 (rotation speed of 18.14RPM). Thus, the only measurements required are the lift, drag and momentum coefficients as a function of angle of attack. Note that these coefficients can also be obtained using X-foil.

Amiet's theory is implemented by using ISVR's in-house fdanoise. An early version of this code accompanies (S Sinayoko, Kingan, and Agarwal 2013) and is available in the public domain under the MIT open source public licence. The new version (commit number 120) is still under development and its source code is currently closed. In comparison to this early version, it is object oriented and implements leading edge noise in addition to trailing edge noise. It has been used in several studies (Samuel Sinayoko, Kingan, and Agarwal 2013; S Sinayoko, Azarpeyvand, and Lyu 2014) and contains several features not used in this work, including an implementation of Howe's model for trailing edge noise for both straight and serrated edges (Howe 1991).

The sound power is computed first by estimating the sound pressure directivity $S_{pp}(\theta, \omega)$ at 100 meters from the hub, using 50 uniformly space observer locations in the mid-plane of the wind turbine, for elevation angles (measured relative to the axis centred on the turbine hub) varying between 0 and 180 degrees. The sound power is then obtained by applying the following formula [???Blandau and Joseph].

$$W(\omega) = \frac{\pi R^2}{\rho_0 c_0} \int_0^\pi S_{pp}(\theta, \omega) F(\theta) \sin \theta \, d\theta, \quad F(\theta) = \frac{\beta^4 \sqrt{1 - M_Z^2 \sin^2 \theta}}{\left(\sqrt{1 - M_Z^2 \sin^2 \theta} + M_Z \cos \theta \right)^2},$$

(4.1)

and its level in decibels is relative to 10^{-12} .

In the measured data, provided by Vestas, the sound power level was obtained from a single measurement of the sound pressure level, 60 meters below the hub and 104.5 meters downstream of the turbine. The conversion from sound pressure level to sound power level was made according to IEC 61400-11. Furthermore, the predicted sound power levels were corrected for atmospheric attenuation, since the measured data was taken at significant distance to the turbine. The atmospheric coefficients were obtained from ISO-96-132 assuming a temperature of 10 degrees and 70% humidity.

5. Results

5.1. Sound power levels

Figure 5.1.1 shows the sound power level (SPWL) for the DAN-AERO wind turbine. Both the measured spectrum (red solid line with triangles) and the computed spectrum (black solid line with diamonds) are presented. The computed spectrum is based on Amiet's theory and is made up of two components. The first component is the trailing edge noise, shown in dashed blue with circles. The second component is the leading edge noise, shown in dashed green with squares. For leading edge noise,

the integral length scale is assumed to be uniform and set to 40m, and the incoming turbulence intensity is set to 12.5%. The overall sound power level (OASPWL) is obtained by summing the powers in each frequency band. The measured OASPWL is 102.5 dBA, compared to 102.2 dBA for the estimated OASPWL. The OASPWL for trailing edge noise only is 101.2 dBA.

Figure 5.1.2 is similar to 5.1.1 and also shows the sound power level, but for varying values of the integral length scale. For each value, the leading edge SPWL is plotted in dashed green, and the corresponding total SPWL, taking into account the trailing edge spectrum shown in 5.1.1, in black. The values taken by the integral length scale are 20m (diamonds), 40m (squares), 80m (circles) and 160m (pentagons). The corresponding OASPWLs in dBA, for the total SPWL (black curves), are 102.5, 102.1, 101.9 and 101.8. The measured SPWL is the red solid line with triangles.

Similarly, figure 5.1.3 varies the turbulence intensity between 5% (diamonds), 12.% (squares) and 20% (circles). The associated OASPWLs are 101.3, 102.2 and 103.4 dBA.

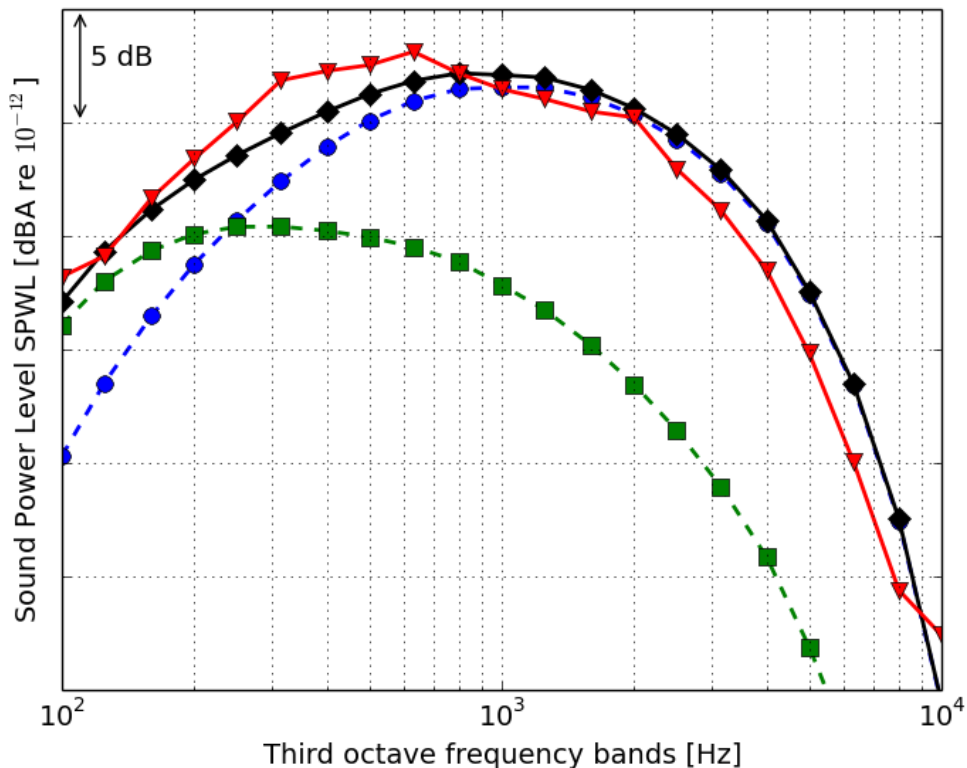


Figure 5.1.1: Measured (red triangles) and predicted (black diamonds) sound power levels (SPWL) in dBA in third octave bands for the DANAERO turbine, using Amiet's model for trailing edge noise (blue circles, dashed) and leading edge noise (green squares, dashed). For leading edge noise, the turbulence intensity and integral length scales are set to 12.5% and 40m. The overall sound power levels in dBA are: 102.5 (measured), 102.2 (predicted), 101.2 (trailing edge only) and 95.3 (leading edge only).

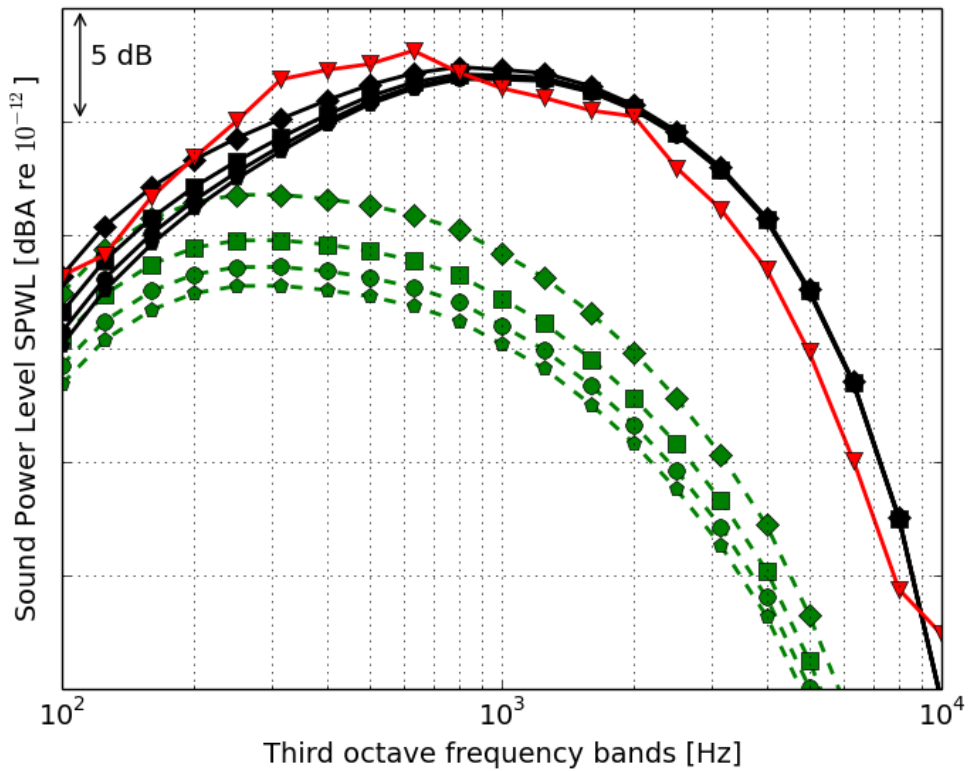


Figure 5.1.2: Impact of integral length scale on sound power level: the green dashed curves give sound power for leading edge noise for an inflow turbulence intensity of 12.5% and an integral length scale of 20m (diamonds), 40m (squares), 80m (circles) and 160 (pentagons). The corresponding total sound powers, including trailing edge noise, are shown in solid black using the same markers. The measured sound power is the solid line with red triangles. Leading edge sound power decreases with integral length scale. The overall sound power levels (black curves) in dBA are: 102.5 (diamonds), 102.1 (squares), 101.9 (circles) and 101.8 (pentagons).

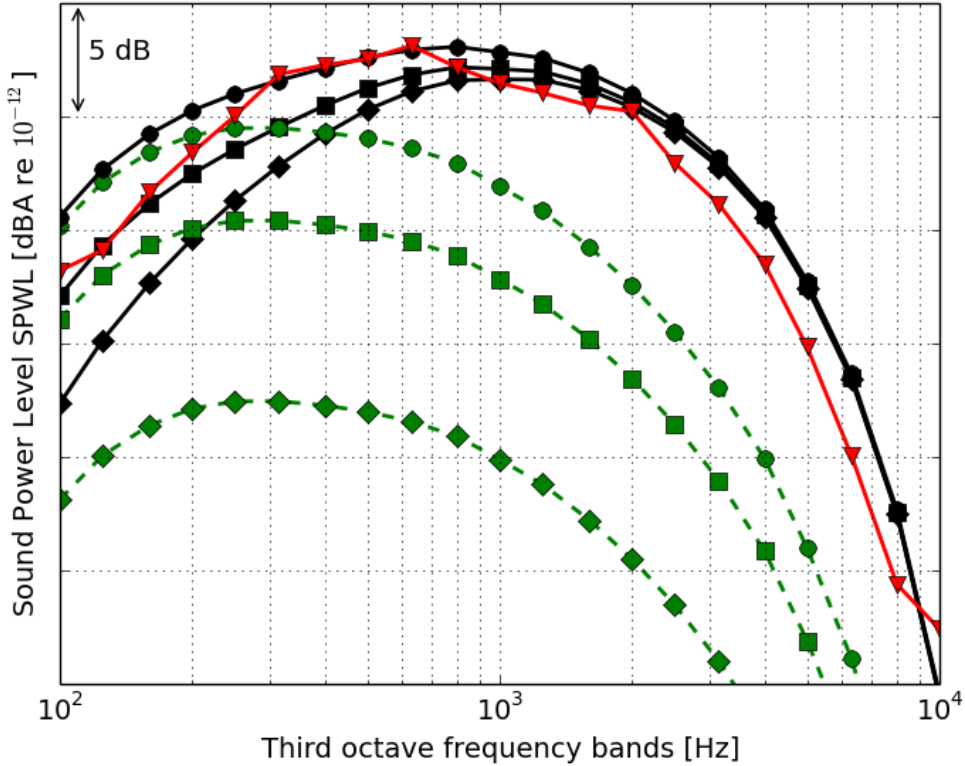


Figure 5.1.3: Impact of turbulence intensity on sound power level: the green dashed curves give sound power for leading edge noise for an integral length scale of 40m and a turbulence intensity of 5% (diamonds), 12.5% (squares) and 20% (circles). The corresponding total sound powers, including trailing edge noise, are shown in solid black using the same markers. The measured sound power is the solid line with red triangles. Leading edge sound power increases with turbulence intensity. The overall sound power levels (black curves) in dBA are: 101.3 (diamonds), 102.2 (squares), 103.4 (circles).

5.2. Amplitude modulation

Figure 5.2.1 presents a map of the amplitude modulation in dBs, estimated using Amiet's model with the same parameters as in figure 5.1.1, around a DAN-AERO wind turbine for: (a) a single bladed rotor; (b) a three bladed rotor. The z-axis gives the position in the flow direction, normalized by the tower height $h = 58m$, with the wind pointing in the negative z direction. The y-axis gives the normalized position in the rotor plane, in the horizontal direction. The map is focused near the turbine, within a radius $R = 2h$ of 116m.

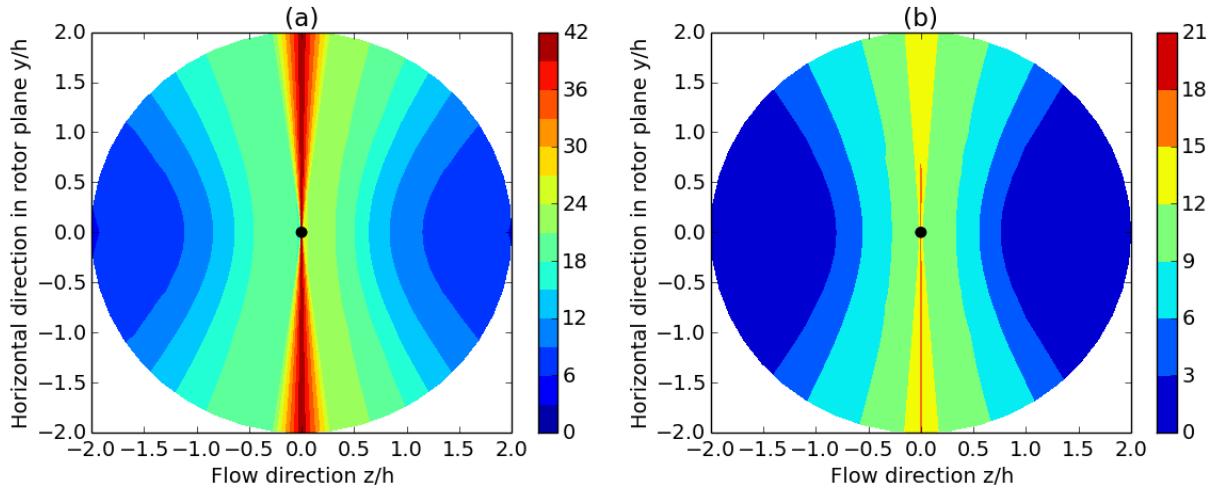


Figure 5.2.1: Amplitude modulation on the ground, in decibels, around a single DANAERO wind turbine estimated using Amiet's model. (a) Single rotating blade (b) Three rotating blades.

Figure 5.2.2 presents a similar map of the amplitude modulation in dBs around: (a) 4 wind turbines; (b) 8 wind turbines. The turbines are equally spaced, with a separation distance between the towers of 194 meters, i.e 3 times the "height plus radius" distance. The map extends further away compared to 5.2.1 to a distance $R = 20h$ of 1160m. The phase of each wind turbine has been randomized so that the instantaneous directivities for each turbines are not synchronized.

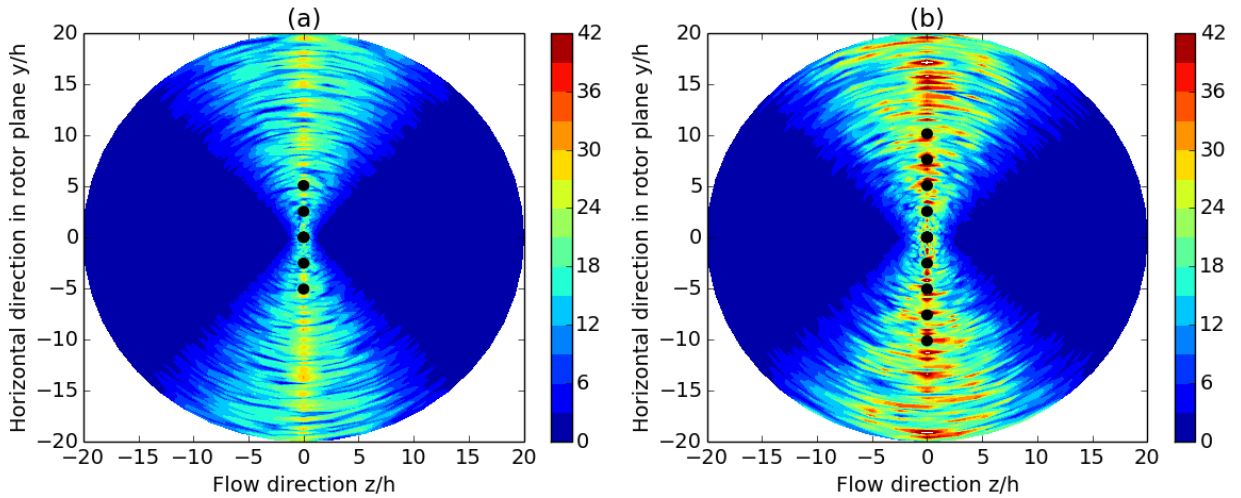


Figure 5.2.2: Amplitude modulation on the ground, in decibels, around multiple DANAERO wind turbines estimated using Amiet's model. (a) 5 turbines (b) 10 turbines.

6. Discussion

6.1. Sound power levels

From figure 5.1.1, the predicted sound power level falls within 3 dBA of the

measurements over the entire frequency range. The prediction underestimates the sound power below 1kHz, and overestimates the sound power otherwise. The predicted overall sound power level (OASPL) of 102.2 dBA is therefore very close to the measured one (102.5 dBA). The difference in the spectra can most likely be explained by our use of the analytical surface pressure spectrum due to (Kim and George 1982), or some error in predicting the spanwise correlation length l_s (equation (3.1.3)), which may be over-estimated at high frequencies. More work is needed to quantify the uncertainty in those two quantities. Figure 5.1.1 also shows that trailing edge noise dominates the sound power except at low frequencies (below 200 Hz in this case), where leading edge noise takes over. The contribution of leading edge noise to the OASPL is only 1.3 dBA in this case. Overall, these preliminary results are encouraging and suggest that Amiet's theory gives reasonable estimates of the sound power level for a full wind turbine, even when using elementary semi-analytical models for the surface pressure spectrum and the correlation length.

In the current study, the integral length scale L and the turbulence intensity I were unknown, so typical values were estimated based on results published by (Glegg, Baxter, and Glendinning 1987). L was assumed to vary between 20m and 160m and the turbulence intensity between 5% and 20%. The effect of each parameter on leading edge noise power, as well as the total sound power is illustrated in figures 5.1.2 and 5.1.3. The leading edge sound power decreases with increasing values of the integral length scale L by 5 dBA. For large values of the L , above 80m, the contribution to the OASPL is small and changes only by -0.1 dBA when doubling L from 80m to 160m. For smaller values of L , changes to the OASPL are more substantial but remain small, with -0.4 dBA for L going from 20m to 40m. In practise, the integral length scale would likely vary with the position of the blade, which has not been taken into account here. However, it appears that the SPWL is relatively insensitive to the value of the integral length scale. The turbulence intensity I has a much large effect, as illustrated in 5.1.3: the SPWL for leading edge noise increases by 12 dBA when increasing I from 5% to 20%. This translates into a contribution to the OASPL of 0.1 dBA to 1.1 dBA and 2.3 dBA. High inflow turbulence intensities, above 10% do have a significant impact on the predicted sound power level. Even if the trailing edge noise levels are predicted accurately, for high inflow turbulence, a good estimate of the inflow turbulence is necessary to predict the OASPL to within 1 dBA.

6.2. Amplitude modulation

Figure 5.2.1(a) gives the amplitude modulation for a single rotating blade. Considering an observer on the ground at 45 degrees to the hub, i.e. for $(z/h, y/h) = (1.0, 0)$, the amplitude modulation experience by the observer is predicted to fall between 10 and 12 dB. This is in line with the typical levels measured by (Sijtsma, Oerlemans, and Holthusen 2001; Oerlemans and Sijtsma 2007) using array measurements. This supports our prediction, although more array measurements are necessary to further validate the prediction. Note that the level of amplitude modulation varies greatly with the observer location. The peak modulation is in the rotor plane, with more than 40 dBA predicted there due to the null in the directivity of the sound in the blade plane. Within zero to about 30 degrees to the rotor plane, the levels of amplitude modulation.

Comparing figure 5.2.1(b) with 5.2.1(a) shows that for a full 3-blade turbine, the amplitude modulation is about very significantly compared to a 1-blade turbine. Thus,

at 45 degrees, the amplitude modulation is less than 3 dB for 3-blades compared to 10-12 dB for a single blade. This is because the instantaneous spectra are out of phase, so the minimum value for one blade does not coincide with the minimum value for another blade. This suggests one simple way of reducing amplitude modulation: to increase the number of rotor blades. However, the modulation levels remain high (12-15 dB) in the rotor plane. Note also that figure 5.2.1(b) is analogous with figure 25 of (Cheong and Joseph 2014), although the amplitude of the modulation appears higher here: Cheong et al predict only 3 dB of swishing near the rotor plane.

In the case of simplified "wind farms", made of equally spaced 3-bladed turbines, figure 5.2.2 shows that the amplitude modulation increases compared to a single turbine. It is less than 3 dB for angles up to 45 degrees to the flow direction. However, in the region around the rotor plane, the amplitude modulation is significant, without about 18 dB within 30 degrees of the rotor plane. There is therefore two distinct regions: a high amplitude modulation region near the rotor plane, and a low modulation region normal to the rotor plane. Doubling the number of turbines increase slightly the size of the noisy region, and increases the magnitude of the modulation by only a few decibels. More work is needed to fully understand the impact of separation distance and blade alignment on wind turbine noise.

7. Conclusions

This paper predicts the sound power level for a DANAERO 40m radius turbine using Amiet's theory for trailing edge and leading edge noise. The predicted overall sound power level agrees very well (less than 0.5 dBA) with measured data. The noise is dominated by trailing edge noise except at low frequencies (less than 200 Hz), where leading edge noise dominates. However, there is some uncertainty on the magnitude of inflow noise. Inflow noise is found to be very sensitive to the level of turbulence intensity, rather than to the size of the integral length scale. If the turbulence intensity is set much higher in the prediction than in the experiment, for example to 20% compared to 10%, then the overall sound power level is over-estimated by up to 1.5 dBA. There is also some uncertainty on the sound power spectrum for trailing edge noise, with low frequencies being under-estimated and high frequencies over estimated by 2-3 dBA. The accuracy may be improved by using improved semi-analytical models tailored to wind turbine blades, such as the TNO-model (Bertagnolio, Madsen, and Bak), or advanced CAA/CFD methods such as synthetic turbulence. Based on these preliminary findings, Amiet's theory appears able to predict the overall sound power level of a full wind turbine to within less than 0.5 dBA when combined with simple surface pressure spectrum models.

The magnitude of amplitude modulation was validated successfully for a single rotating rotor: it matches the expected 10-12 dB modulation in sound pressure level near the ground at 45 degrees to the hub. More experimental array measurements are needed to further validate the predictions. Most importantly, amplitude modulation greatly reduces when considering a full wind turbine, compared to only a single blade. For an observer on the ground at 45 degrees to the hub, the predicted amplitude modulation is less than 3 dB. However, amplitude modulation in the rotor plane is a major concern, with predicted amplitudes of up to 10-15 dBA. The predicted amplitude modulation is qualitatively consistent with the results of Cheong et al, although the levels predicted in this study appear higher in the rotor plane. Finally, the amplitude modulation extends to a wide range of angles (up to 30-40

degrees) around the rotor plane, which increases the number of wind turbines aligned within that plane. More research is needed to understand the effect of separation distance and turbine alignment on amplitude modulation.

Acknowledgements

The first author wishes to gratefully acknowledge the financial support of the Royal Commission of 1851, as well as Dr Anurag Agarwal and Mitsubishi Heavy Industries, for funding preliminary work on wind turbine noise at the University of Cambridge. The authors also thank Professor Phil Joseph for many fruitful discussions on this manuscript.

- Amiet, R. 1975. "Acoustic Radiation from an Airfoil in a Turbulent Stream." *Journal of Sound and Vibration* 41 (4): 407–20. doi:10.1016/S0022-460X(75)80105-2.
- . 1976. "Noise due to Turbulent Flow Past a Trailing Edge." *Journal of Sound and Vibration* 47 (3): 387–93. doi:10.1016/0022-460X(76)90948-2.
- Amiet, R K. 1976. "High Frequency Thin-Airfoil Theory for Subsonic Flow." *AIAA Journal* 14: 1076–82.
<http://www.csa.com/partners/viewrecord.php?requester=gs&collection=TRD&recid=A7641697AH>.
- . 1986. *Leading and Trailing Edge Noise from a Helicopter Rotor. Analysis*.
- Amiet, RK. 1978. "Effect of the Incident Surface Pressure Field on Noise due to Turbulent Flow Past a Trailing Edge." *Journal of Sound and Vibration* 57: 305–6.
<http://www.csa.com/partners/viewrecord.php?requester=gs&collection=TRD&recid=A7832785AH>.
- Bertagnolio, Franck, Helge Aa Madsen, and Christian Bak. *Experimental Validation of TNO Trailing Edge Noise Model and Application to Airfoil Optimization*.
- Brooks, T. F., and T. H. Hodgson. 1981. "Trailing Edge Noise Prediction from Measured Surface Pressures." *Journal of Sound and Vibration* 78: 69–117.
<http://www.sciencedirect.com/science/article/pii/S0022460X81801587>.
- Casper, J, and F Farassat. 2004. "Broadband Trailing Edge Noise Predictions in the Time Domain." *Journal of Sound and Vibration* 271 (1-2): 159–76.
doi:10.1016/S0022-460X(03)00367-5.
- Cheong, Cheolung, and Phillip Joseph. 2014. "Cyclostationary Spectral Analysis for the Measurement and Prediction of Wind Turbine Swishing Noise." *Journal of Sound and Vibration* 333 (14). Elsevier: 3153–76. doi:10.1016/j.jsv.2014.02.031.
- Curle, N. 1955. "The Influence of Solid Boundaries upon Aerodynamic Sound." *Proceedings of the Royal Society of London A* 231 (1187): 505–14.
<http://rspa.royalsocietypublishing.org/content/231/1187/505.short>.

- Ffowcs-Williams, J E. 1963. "The Noise from Turbulence Convected at High Speed." *Philosophical Transactions for the Royal Society of London. Series A, Mathematical and Physical Sciences* 255 (1061): 469–503.
- Glegg, SAL, SM Baxter, and AG Glendinning. 1987. "The Prediction of Broadband Noise from Wind Turbines." *Journal of Sound and Vibration* 118 (2). Elsevier: 217–39. <http://linkinghub.elsevier.com/retrieve/pii/0022460X87905220>.
- Howe, M S. 1978. "A Review of the Theory of Trailing Edge Noise." *Journal of Sound and Vibration* 61 (3): 437–65. doi:10.1016/0022-460X(78)90391-7.
- . 1991. "Noise Produced by a Sawtooth Trailing Edge." *The Journal of the Acoustical Society of America* 90 (1): 482–87. doi:10.1121/1.401273.
- Kim, Y N, and a. R George. 1982. "Trailing-Edge Noise from Hovering Rotors." *AIAA Journal* 20 (9): 1167–74. doi:10.2514/3.51176.
- Lee, Seunghoon, Seungmin Lee, and Soogab Lee. 2013. "Numerical Modeling of Wind Turbine Aerodynamic Noise in the Time Domain." *The Journal of the Acoustical Society of America* 133 (2): EL94–100. doi:10.1121/1.4774072.
- Lowson, M V. 1993. "A New Prediction Model for Wind Turbine Noise." In *Renewable Energy - Clean Power 2001, 1993., International Conference on*, 177–82.
- Madsen, Helge Aagaard, Christian Bak, Uwe Schmidt Paulsen, Mac Gaunaa, Risø Dtu, Peter Fuglsang, L M Glasfiber, et al. 2010. *The DAN-AERO MW Experiments Final Report Risø-R-Report*. Vol. 1726. doi:978-87-550-3809-7.
- Moreau, Stéphane, and Michel Roger. 2009. "Back-Scattering Correction and Further Extensions of Amiet's Trailing-Edge Noise Model. Part II: Application." *Journal of Sound and Vibration* 323 (1-2): 397–425. doi:10.1016/j.jsv.2008.11.051.
- Oerlemans, S. 2009. "Detection of Aeroacoustic Sound Sources on Aircraft and Wind Turbines." University of Twente. <http://doc.utwente.nl/67363/>.
- Oerlemans, S, and J G Schepers. 2010. "Prediction of Wind Turbine Noise and Validation against Experiment." *Noise Notes* 9 (2): 3–28. <http://dx.doi.org/10.1260/1475-4738.9.2.3>.
- Oerlemans, S, and P Sijtsma. 2007. "Location and Quantification of Noise Sources on a Wind Turbine." *Journal of Sound and Vibration* 299 (4-5): 869–83. <http://linkinghub.elsevier.com/retrieve/pii/S0022460X06006316>.
- Roger, M, and S Moreau. 2005. "Back-Scattering Correction and Further Extensions of Amiet's Trailing-Edge Noise Model. Part 1: Theory." *Journal of Sound and Vibration* 286 (3): 477–506. doi:10.1016/j.jsv.2004.10.054.
- Roger, Michel, and Stéphane Moreau. 2012. "Addendum to the Back-Scattering Correction of Amiet's Trailing-Edge Noise Model." *Journal of Sound and Vibration* 331 (24): 5383–85. doi:10.1016/j.jsv.2012.06.019.

- Schlinker, Robert H, and Roy K Amiet. 1981. *Helicopt. Science News*. Vol. 119.
- Sijtsma, P, S Oerlemans, and H Holthusen. 2001. *Location of Rotating Sources by Phased Array Measurements*. Aerospace. National Aerospace Laboratory NLR. <http://www.nlr.nl/id~4369/l~en.pdf>.
- Sinayoko, S, M Azarpeyvand, and B Lyu. 2014. "Trailing Edge Noise Prediction for Rotating Serrated Blades." In *20th AIAA/CEAS Aeroacoustics Conference, Aviation 2014, Atlanta, USA, 16--20 June 2014*.
- Sinayoko, S, M Kingan, and A Agarwal. 2013. "Trailing Edge Noise Theory for Rotating Blades in Uniform Flow." *Proceedings of the Royal Society A: Mathematical, Physical and Engineering Science* 469 (2157): 20130065. doi:10.1098/rspa.2013.0065.
- Sinayoko, Samuel, Michael Kingan, and Anurag Agarwal. 2013. "On the Effect of Acceleration on Trailing Edge Noise Radiation from Rotating Blades." In . American Institute of Aeronautics and Astronautics. doi:10.2514/6.2013-2287.